Review Article

Interplay effect in lung cancer proton therapy

Jun Hao Phua, Khong Wei Ang

National Cancer Centre Singapore, 169610, Singapore

Contributions: (I) Conception and design: All authors; (II) Administrative support: All authors; (III) Provision of study materials or patients: All authors; (IV) Collection and assembly of data: All authors; (V) Data analysis and interpretation: All authors; (VI) Manuscript writing: All authors; (VII) Final approval of manuscript: All authors.

Correspondence to: Jun Hao Phua. National Cancer Centre Singapore, 11 Hospital Drive, 169610, Singapore. Email: phua.jun.hao@nccs.com.sg.

Abstract: Pencil beam scanning proton therapy is used increasingly for cancer treatment. Although this technique allows superior dose avoidance to critical organs in comparison to passive scattering and X-rays photon-type radiation therapy, it is more susceptible to changes in the patient's inherent anatomical motion, especially in the thoracic region. The uncertainties in dose distribution due to motion interplay in this region are significant and cannot be ignored. This paper focuses on the errors in dose delivery when motion interplay is involved, and how we can quantify them practically. With the proper tools for evaluating the magnitude of such errors, the best method to mitigate motion effects can be decided and designed for each individual patient.

Keywords: Proton therapy; pencil beam scanning; motion interplay

Received: 31 January 2018; Accepted: 19 November 2018; Published: 11 December 2018.
doi: 10.21037/jxym.2018.11.04
View this article at: http://dx.doi.org/10.21037/jxym.2018.11.04

Introduction

Due to the advances in technology, the treatment of tumours using radiation has become very localised or conformal, even at sites that see higher potential of motion, for example lung. With intensity modulated radiation therapy (IMRT) and intensity modulated arc therapy (IMAT), the conformality of treatment has improved (1,2). With the advent of proton therapy, the dose received by the organs at risk can be lowered or controlled while not compromising the intended target dose (3-5), giving clinicians the option to further escalate treatment dose.

Tackling the problem of motion during treatment would be the logical approach to ensure quality of the treatment plan is not compromised during patient delivery. Some mitigation methods are as presented in the table, along with its purpose (*Table 1*).

However, the above methods cannot be applied to the same class of treatment routinely. The best method should be decided and designed for each individual patient. It is therefore important to fully understand the dynamics of the motions involved before a sound decision can be made.

The subject of motion interplay has been studied extensively in the context of radiation therapy using high energy X-ray (8,9). In particular, the two main types of motions are: (I) motion of the tumour and body parts; (II) motion of the multi-leaf collimators (MLCs) forming the different windows during IMRT or IMAT irradiations. Each of the motion has to be understood and modelled individually before being integrated to derive their composite or interplay effect. A comprehensive knowledge of these effects allows precise determination of dose deposition probability to any position within the tumour and the OARs.

This is even more important for proton therapy, due to the sharp dose fall-off at the end of the Bragg peak (10-12), which will be described in more detail in the following section.

This review paper aims to highlight the uncertainties involved in lung proton therapy due to motion interplays, and how we can quantify them practically.

Table 1 Table describing the different techniques of motion management and the principles

No.	Techniques by industrial name	How is it performed
1	Breath-hold	Stop or limit the motion of the tumour. Patient holds breath for the period of beam on
2	Amplitude gating	The beam is only delivered when the tumour moves to within the range of the desired position. Patient breathes normally
3	Real-time tracking and irradiation (6)	Motion of the tumour is tracked, and the beam goes to the predicted position of the tumour. The beam is then delivered at that position when the tumour reaches the position
4	Internal tumour volume (ITV) treatment (7)	A bigger treatment volume which encompasses the whole trajectory of the tumour positions and the whole volume is then treated as a static target

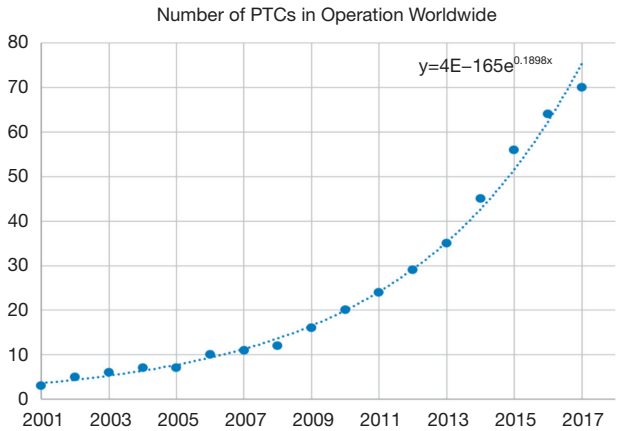

Figure 1 Number of proton therapy centres in operation worldwide from 2001 to 2017. Data from PTCOG (14). The curve shows an exponential increase.

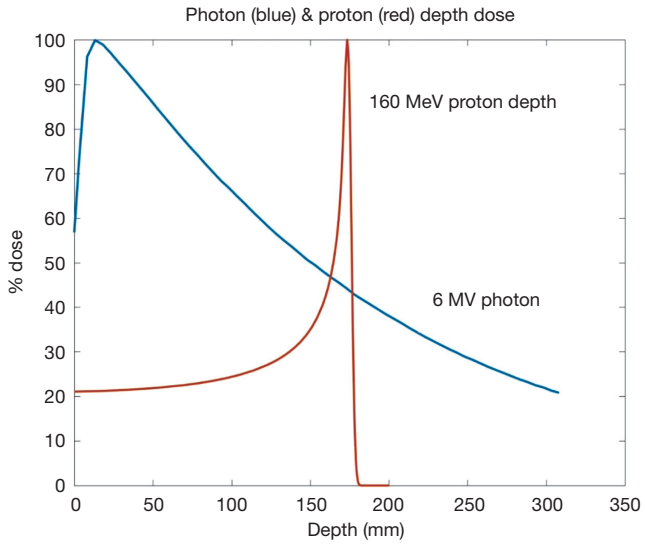

Figure 2 Measured data showing a 160 MeV proton Bragg peak and a 6 MV X-rays photon depth distribution. Note the sharp gradient of the Bragg peak compared to the photon's more gradual fall-off.

Brief outline of proton therapy with pencil beam scanning

Proton therapy has been introduced to the world of radiation therapy since the 1950s (13). However, due to limitations of accelerator and magnet technology, traditional proton therapy machines were large, measuring several metres in width and height, and weighing hundreds of tons (14). Proton therapy is not widely used only until the early 2000s. A proton therapy machine has also become more affordable with the maturation of the technology, leading to an increase in Proton Therapy machine being constructed in hospital. Between 2010 and 2017, 50 new proton therapy facilities were started (15) (*Figure 1*).

The promise of proton therapy lies heavily on the existence of a Bragg peak, a narrow region where the dose deposition peaks and falls off sharply as shown in *Figure 2*. Protons with higher energies deposit their maximum dose at greater depths. By accumulating weighted dose depositions over a range of proton energies, a spread-out Bragg peak (SOBP) can be obtained. This is shown in *Figure 3*, where the proportion of proton fluence with energies 139, 137, 131, and 125 MeV are 0.32, 0.28, 0.23 and 0.17 respectively. Using more energies between the range 125 to 137 MeV, a more uniform "flat top" depth dose can be attained. By designing proper beam entries, a very conformal dose distribution can be achieved using proton therapy, with sufficiently coverage of the clinical tumour volume (CTV), and minimal dose to the OARs which are beyond the range of the maximum energy protons (16,17). An example is as shown in *Figure 4*.

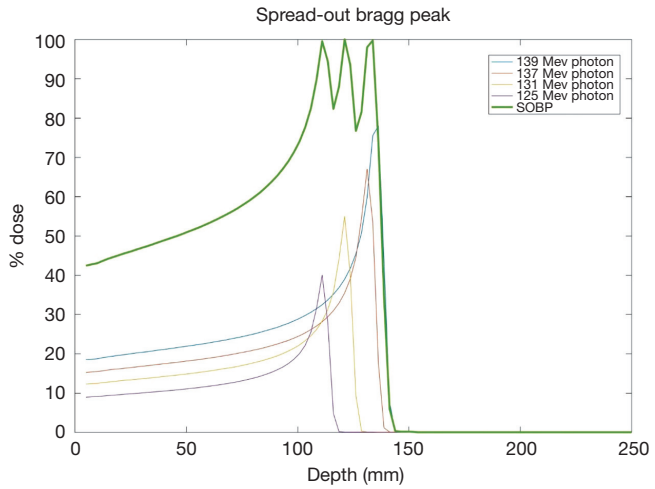

Figure 3 Curves showing formation of SOBP from a superposition of different energy Bragg peaks. The proportion of fluence for 139, 137, 131 and 125 MeV protons is 0.32, 0.28, 0.23 and 0.17 respectively. SOBP, spread-out Bragg peak.

Passive scattering and pencil beam scanning (PBS) are the two main techniques used in proton beam delivery (10,14).

In passive scattering nozzle, a beam of protons passes through a rotating, variable-thickness-modulating scatterer (the range modulation wheel in *Figure 5*) to spread the beam in the z-direction, then passes a second scatterer downstream to further spread the beam laterally in the x-y direction. This results in a 3-dimensional box volume analogous to X-rays' 3-D conformal radiation therapy (3DCRT).

In PBS nozzle, a sharp pencil beam of protons is deflected over x-y directions using magnetic fields (10,14,18,19). Every beam has a finite beam spot size (typically millimetres in dimensions) with fluence that is Gaussian distributed. The beam is swept laterally orthogonal to the beam direction. To create dose deposition at varying depth of the target, the proton beam energy is changed while maintaining the lateral scanning. A superposition of all the pencil beams therefore creates a 3-D dose distribution (*Figure 6*).

Although passive scattering currently dominates clinical use, PBS is the more advanced technology and it is becoming the preferred choice for new centres (10,14). The reason is PBS allows for the delivery of intensity modulated proton therapy (IMPT) which allows for greater dose conformity similar to IMRT in photons radiation therapy (17).

Motion interplay effects

Highly conformal doses are deposited to the stationary target by the proton pencil beam scanning. Interplay effect is observed as the dose deposition happen when the target moves. It results in a sub-optimal dose distribution contributed by the lack of synchronization between the beam delivery and the desired target position. Steep dose gradients are planned for between the target volume and the normal tissue, thus when the target moves, interplay will result in dose degradation, such as, regions of over-dosage and under-dosage, in comparison with the 'static' treatment plan.

As shown in *Figure 7*, the target is simulated to move diagonally in a periodic manner, while a particle beam sweeps across left to right and top to bottom. Some parts of the tumour get irradiated only when it crosses the path of the sweeping pencil beam. This will result in regions of over-dose and under-dose (20).

4D composite dose

A mathematical framework can be set up to quantify interplay dosimetric effects (21). In general, the 4D composite dose model can be written as

$$Dm(r) = \int Do(r - r') \cdot (r')dr' \quad [1]$$

$Dm(r)$ is the modified dose distribution at position r. $Do(r-r')$ is the original reference plan dose distribution at position $r-r'$. $P(r')$ is the probability density function describing the target motion due to breathing. Eq. [1] is integrated over all the positions r' of the target's trajectory.

The breathing pattern can be described by

$$Z(t) = Zo - b \cdot \cos^{2n}(\frac{\pi t}{t} - \varphi) \quad [2]$$

Zo is the position at exhale, b is the amplitude of the motion, $Zo-b$ is the position at inhale, τ is the period of breathing cycle, n is a parameter that determines general shape of the breathing model, and φ is the starting phase of the breathing cycle.

$P(r')$ can be expressed as a function of position as derived from [2,3]

$$P(r')dr = \frac{dt}{\left(\frac{\tau}{2}\right)} \quad [3]$$

In a single dimension,

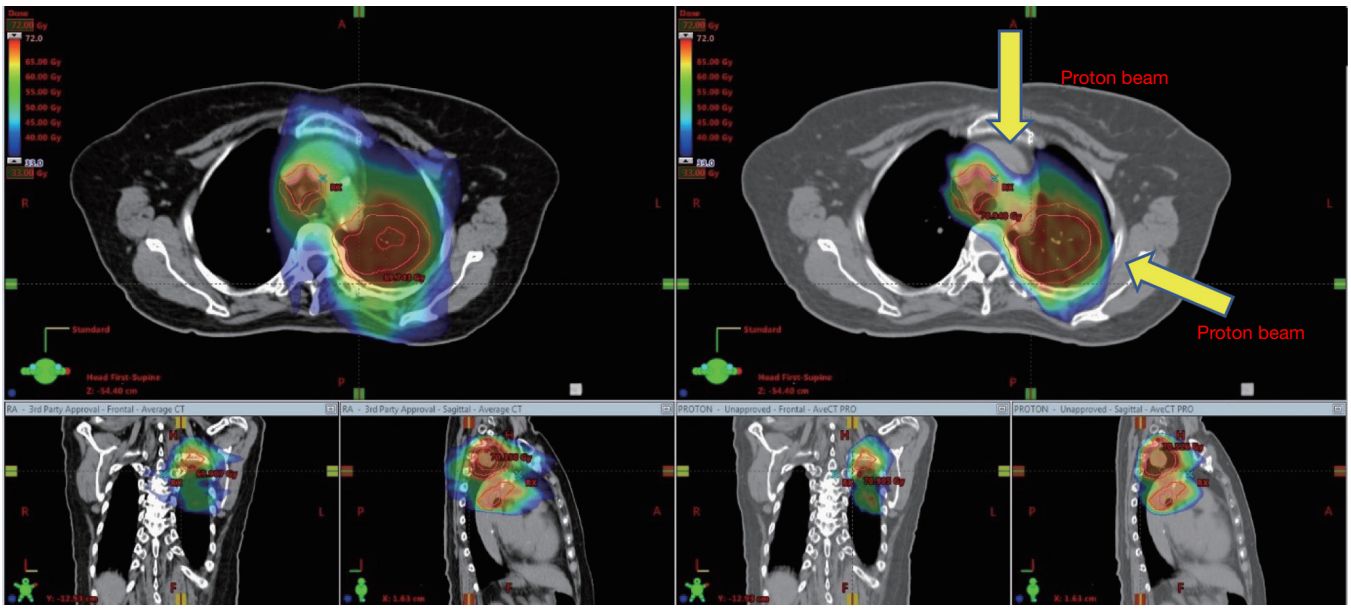

Figure 4 Dose distribution comparison between IMAT (left) and proton therapy (right) for lung radiation therapy. The proton therapy potentially deposits less dose to the OAR (spinal cord) as compared to the IMAT. IMAT, intensity modulated arc therapy.

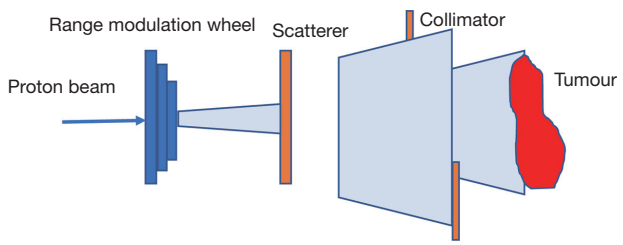

Figure 5 Conceptual schematic of a passive scattering proton system.

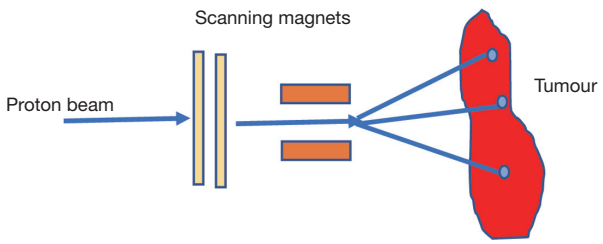

Figure 6 Conceptual schematics of a pencil beam scanning system.

$$P(z)=1/\left[n\cdot b\cdot\pi\cdot\left(\frac{Zo-Z}{b}\right)^{\frac{2n-1}{2n}}\cdot\left\{1-\left(\frac{Zo-Z}{b}\right)\frac{1}{n}\right\}^{\frac{1}{2}}\right] \quad [4]$$

for $Zo-b<Z<Zo$

For the above form to be completely true requires integration over infinite number of fractions and breathing cycles.

In practice, this can be achieved approximately, for conventional fractionated treatments of typically 30 fractions of 2 Gy each. Furthermore, each beam-on time takes minutes which involves a lot of cycles. Thus, interplay effect is more significant in hypo-fractionated SBRT/SRS type cases (22).

Measurements on Interplay effects with Proton Scanning Beam

The measurements on the interplay effect are best presented by Bert *et al.* in 2008 (20) and Ciocca *et al.* in 2016 (23). In Bert's paper, square fields of 110 mm defined by a 50% isodose line are irradiated with monoenergetic protons (spot size 8 mm FWHM) and measured using films. An amplitude of 8 to 20 mm, period of 3–7 s per cycle, and starting phase from 0 to 270 degrees are used as variables. A static target is first covered by a planned static dose distribution which forms the reference irradiation measurement. The dose distributions with motion interplay are then compared with the reference measurement to show

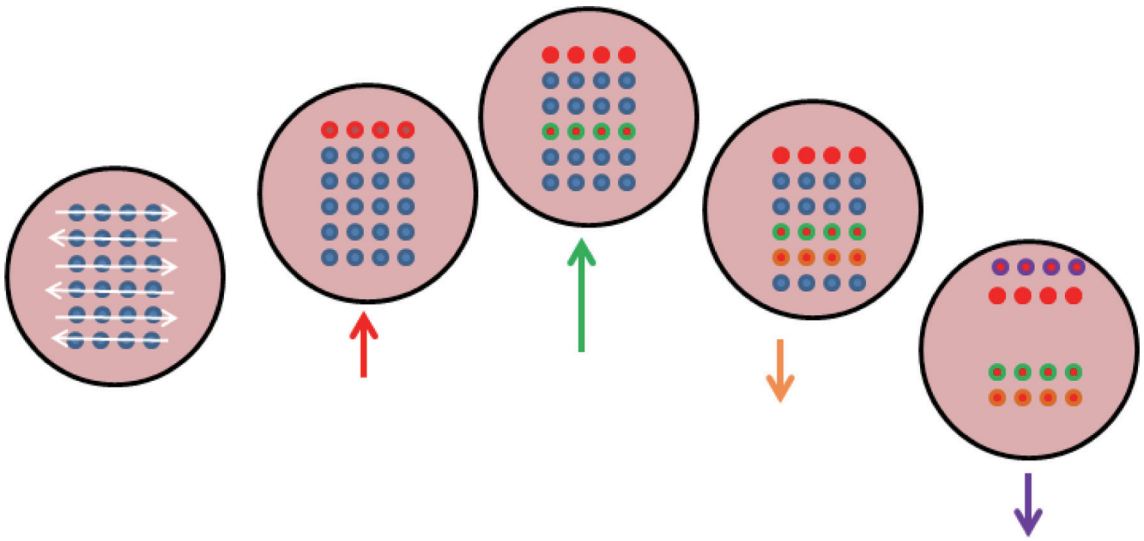

Figure 7 Sequence showing beam and target motion interplay. The red spots represent the parts that receive irradiation. The pink circle represents the target moving, with the intended dose delivery distribution represented by the blue circles, with the beam scanning direction represented by the white arrows. As the target moves with the direction of the arrow indicated green, yellow and purple, the dose received by the target is represented by the red filling, with the colour of the directional arrow outlined. The final dose distribution is represented by the last circle showing the deteriorated dose distribution

the random 'hot' and 'cold' spots after irradiation.

Comparing across films with the same starting phase and breathing period shows that interplay effects worsen with increasing amplitudes. It was observed that this is true regardless of starting breathing phase. Comparing measurements of motion with the same amplitude and breathing period but different starting phases further shows that tumour starting position did not affect the interplay effects. In conclusion, amplitude seems to play a more significant role. In that paper, it was observed that interplay effects also worsen with slower breathing. It was observed that the local over- and under-dose is "smeared out". This could be due to mismatch in timing of breathing and beam scanning speed.

In another measurement, the film is moved vertically and horizontally respectively (20), while the beam scanning takes place horizontally. It is observed that the interplay effect is significantly inferior when the direction of target motion is perpendicular to the scanning beam.

Finally, a metallic screw is irradiated with proton beams, and the proton radiograph image of the screw is captured on film (23). The static screw showed up as a sharp image. The moving screw images appear blurred due to interplay effects (23).

Theoretical simulations of interplay effects with proton pencil scanning beam

Due to the many scenarios that may occur, measurements to quantify and understand interplay effects may not be practical in a busy clinic. A simulation may be a good tool to use for evaluating whether interplay effects are important before treatment. To the best of the authors' knowledge, at this time of writing, there is no one integrated commercial treatment planning system that can perform such simulations. In-house developments should be encouraged and validated.

The general work flow to investigate the effects of interplay is outlined as follows:

(I) Image a patient using 4DCT with a proper respiratory surrogate signal.

(II) Create a static reference plan which delivers a dose to an internal tumour volume ITV that incorporates the full trajectory of the tumour volume calculated to a static patient CT with averaged Hounsfield units derived from the 4DCT.

(III) Create a plan, based on the reference treatment plan that maps the dose delivered to the different phases of a 4DCT image to a static reference phase

image, and summing up these doses. This simulates delivering dose to a moving patient anatomy.

The dose distributions of [I] and [III] will be evaluated and compared.

The following sub-sections further describe each part of the work flow.

4DCT imaging

The use of 4DCT for imaging moving tumours has become an industry standard since it is commercially available in 2002 (24). In principle, 4DCT image acquisition is the real-time recording of a respiratory signal simultaneously with image over-sampling. By re-imaging the same anatomy at different respiratory positions, a sufficient quantity of CT slices allows respiratory sorting with acceptable spatial accuracy. The over-sampled images from the CT dataset are then sorted into several bins or phases, based on the information obtained from the respiratory signal. A 4DCT dataset is then a complete set of image bins acquired over a respiratory cycle (24). Various commercial systems such as RPM (Varian Medical Systems, Inc.) and Abches III (APEX Medical, Inc.) can be used to obtain the respiratory signal.

The 4DCT dataset normally includes 10 sets of images from the 10 phases of breathing in a cycle, CT0% to CT90%. The end-exhalation phase is usually CT50%, while CT0% and CT90% are end-inhalation phases. Each phase will show the tumour at different positions. An average of all the images from the 10 phases gives an average CT image which incorporates smeared out motion artefacts. This image is typically used in radiation therapy for dose calculation to a pseudo moving patient.

Static reference treatment plan

The generic workflow of treatment involving tumour in motion for megavoltage X-ray treatment is as followed (25,26):

(I) GTV from each respiratory phase of the 4DCT is used to generate the ITV that encloses all of the identified GTVs.

(II) A uniform expansion margin is applied to the ITV to obtain the PTV.

(III) The plan is then robust optimized such that the dose covers the ITV.

This described technique can be extended to proton scanning beam therapy.

Calculation of 4D composite dose

A practical solution to the 4D composite dose calculation could be as follows:

(I) Use all 10 respiratory phases' images for dose calculations.

(II) Based on the specifications of the proton delivery system the beam on timing for each spot needs to be determined. The spots list from the reference plan, partition and assign each spot to its corresponding respiratory phase.

(III) With 10 sets of beam spots assigned to each image CT0% to CT90%, the dose delivered to each GTV is calculated.

(IV) In order to accumulate the dose delivered to the patient, all the spatial voxels' dose in each respiratory phase must be mapped into a reference dataset and summed up. Usually the CT50% phase image is chosen as the reference image. 2 mapping strategies are described in the next section.

(V) Various scenarios are calculated by repeating (I) to (IV) each with different starting phases, simulating different starting tumour locations. The probability of each starting phase is determined. This probability is used to modulate the weightage of each scenario in the final accumulation.

Dose mapping strategies for 4D dose accumulation

For accurate dose accumulation, there must be good correlation of anatomy structures between the source and target voxels. This can be achieved by generating the displacement vector field (DVF) through deformable image registration (DIR). Commercial products available for deformable registration are MIM Maestro (MIM Software Inc., Cleveland, OH, USA), or, Velocity (Varian Medical Systems, Inc.).

The DIR is performed on the image grid, while the radiation dose is calculated on the dose grid separately. Values from the dose grid must be transferred to the image grid and assigned to the anatomy structures there. Direct dose mapping is one method for performing such dose transfer. Using the DVF, dose value from every source voxel is directly transferred to the corresponding target voxel. However, because the dose and image grids are independent and usually their voxel centres do not overlap, such direct transfer using DVF often result in a target voxel receiving

dose from more than one source voxel.

The energy-mass transfer (EMT) (27) algorithm takes care of the overlaps in dose transfer. The mass as well as the energy of each source voxel is determined. They are transferred to the target voxel based on the DVF. The total energy in each target voxel is divided by the mass it receives to give the dose value. This method follows strictly the definition of dose.

The DDM and EMT algorithms produced markedly different cumulative dose in regions with sharp mass-density discrepancies or high dose gradients. The EMT should be used as it is a more physically sound model of dose transfer (27).

Comparison and evaluation of 4D dose distribution and static reference dose distribution

Studies from various groups based on variations of the above-mentioned strategy had been documented.

Bert *et al.* showed that for particle beam therapy, interplay of scanned beams and moving targets severely affected planned dose distributions. Fractionated treatment delivery potentially mitigates at least parts of these interplay effects (14). This supported results from Bortfeld, Chui, Jiang and Schaefer (9,28-30) who had shown that interplay effects in IMRT can be smoothened with multiple fields and a large number of fractions. The standard deviation of the dose distribution is within 1% of the mean. Hypo-fractionated lung SBRT studies by Zou *et al.* showed that the tumour volume coverage is not significantly different between static and dynamic simulation, however, for OARs that are close to the target, large dose variations were noted (22). However, Bert found that hypo-fractionated treatment of moving targets with scanned particle beams requires motion mitigation techniques (21). Kardar *et al.* reported that interplay effects can be mitigated by increasing the number of iso-layered re-scanning in each fraction (31).

Conclusions

When scanning proton beam treatment delivery involves motion interplay, the planned dose distribution is deteriorated. The extent or amplitude of the motion plays a significant role in this interplay; thus, it is important that motion is reduced or mitigated. However, treatments with large fractionations will help to average out the hot and cold spots caused by motion interplay. Awareness of these effects allows clinicians and their dosimetry teams to design proper treatment strategies, for example, re-scanning the tumour region by splitting each single field into multiple fields within the same fraction. It may be worth investing in simulation tools development. A proper tool for evaluation of motion interplay effects on any single patient will give confidence in the treatment prescribed.

Acknowledgements

Thank Hong Qi Tan for his invaluable comments and proof-reading.
Funding: None.

Footnote

Provenance and Peer Review: This article was commissioned by the Guest Editors (Kam-Weng Fong, Kevin Lee Min Chua) for the series "Radiotherapy in Lung Cancer" published in *Journal of Xiangya Medicine*. The article has undergone external peer review.

Conflicts of Interest: Both authors have completed the ICMJE uniform disclosure form (available at http://dx.doi.org/10.21037/jxym.2018.11.04). The series "Radiotherapy in Lung Cancer" was commissioned by the editorial office without any funding or sponsorship. The authors have no other conflicts of interest to declare.

Ethical Statement: The authors are accountable for all aspects of the work in ensuring that questions related to the accuracy or integrity of any part of the work are appropriately investigated and resolved.

References

1. Narayanasamy G, Granatowicz D, Baacke D, et al. A Comparison between Three-Dimensional Conformal Radiotherapy, Intensity-Modulated Radiotherapy, and

Volumetric-Modulated Arc Therapy Techniques for Stereotactic Body Radiotherapy of Lung Tumors. Int J Med Phys Clin Eng Radiat Oncol 2015;4:104-12.
2. Boyle J, Ackerson B, Gu L, Dosimetric advantages of intensity modulated radiation therapy in locally advanced lung cancer. Adv Radiat Oncol 2017;2:6-11.
3. Hernandez M, Zhang R, Sanders M, A treatment planning comparison of volumetric modulated arc therapy and proton therapy for a sample of breast cancer patients treated with post-mastectomy radiotherapy. J Proton Ther 2015;1:119.
4. Diwanji T P, Mohindra P, Vyfhuis M, et al. Advances in radiotherapy techniques and delivery for non-small cell lung cancer: benefits of intensity-modulated radiation therapy, proton therapy, and stereotactic body radiation therapy. Transl Lung Cancer Res 2017;6:131-47.
5. Chi A, Lin LC, Wen S, et al. Comparison of photon volumetric modulated arc therapy, intensity modulated proton therapy, and intensity modulated carbon ion therapy for delivery of hypo-fractionated thoracic radiotherapy. Radiat Oncol 2017;12:132.
6. Keall PJ, Mageras GS, Balter JM, et al. The management of respiratory motion in radiation oncology, Report of AAPM Task Group 76. Med Phys 2006;33:3874-900.
7. Vedam SS, Keall PJ, Kini VR, et al. Acquiring a four-dimensional computed tomography dataset using an external respiratory signal. Phys Med Biol 2003;48:45-62.
8. Seco J, Sharp GC, Turcotte J. Effects of organ motion on IMRT treatments with segments of few monitor units. Med Phys 2007;34:923-34.
9. Bortfeld T, Jokivarsi K, Goitein M, et al. Effect of intra-fraction motion on IMRT dose delivery: Statistical Analysis and Simulation. Phys Med Biol 2002;47:2203-20.
10. Liu H, Chang JY. Proton therapy in clinical practice. Chinese Journal of Cancer 2011;30:315-26.
11. Therapy with Protons and Ion Beams, 2012/13. Available online: http://www.desy.de/~garutti/LECTURES/BioMedical/Lecture2_TherapyProtonsIons.pdf
12. Newhauser WD, Zhang R. The physics of proton therapy. Phys Med Biol 2015;60:R155.
13. History of Proton Therapy. Available online: https://www.mdanderson.org/patients-family/diagnosis-treatment/care-centers-clinics/proton-therapy-center/what-is-proton-therapy/history-of-proton-therapy.html
14. Wang D. A critical appraisal of the clinical utility of proton therapy in oncology. Med Devices (Auckl) 2015;8:439-46.
15. Proton Therapy Cooperative Group (PTCOG). Available online: https://www.ptcog.ch/index.php/facilities-in-operation
16. Jones B. The case for particle therapy. Br J Radiol 2006;79:24-31.
17. Lomax AJ, Boehringer T, Coray A, et al. Intensity modulated proton therapy: A clinical example. Med Phys 2001;28:317-24.
18. Paganetti H. editor. Proton Therapy Physics (Series in Medical Physics and Biomedical Engineering). CRC Press, 2011.
19. Marchand B, Prieels D, Bauvir B. IBA Proton Pencil Beam Scanning: An Innovative Solution For Cancer Treatment. Proceedings of EPAC. 2000, Vienna, Austria.
20. Bert C, Grözinger SO, Rietzel E. Quantification of interplay effects of scanned particle beams and moving targets. Phys Med Biol 2008;53:2253-65.
21. Lujan AE, Larsen EW, Balter JM, et al. A method for incorporating organ motion due to breathing into 3D dose calculations. Med Phys 1999;26:715-20.
22. Zou W, Yin L, Shen J, et al. Dynamic simulation of motion effects in IMAT Lung SBRT. Radiat Oncol 2014;9:225.
23. Ciocca M, Mirandola A, Molinelli S, et al. Commissioning of the 4-D treatment delivery system for organ motion management in synchrotron-based scanning ion beams. Physica Medica 2016;32:1667-71.
24. Ehrhardt J, Lorenz C. editors. 4D Modeling and Estimation of Respiratory Motion for Radiation Therapy, Biological and Medical Physics, Biomedical Engineering. Springer, 2013:Chapter 1.
25. Guckenberger M, Wilbert J, Krieger T, et al. Four-dimensional treatment planning for stereotactic body radiotherapy. Int J Radiat Oncol Biol Phys 2007;69:276-85.
26. Tian Y, Wang Z, Ge H, et al. Dosimetric comparison of treatment plans based on free breathing, maximum, and average intensity projection CTs for lung cancer SBRT. Med Phys 2012;39:2754-60.
27. Li HS, Zhong H, Kim J, et al. Direct Dose Mapping Versus Energy/Mass Transfer Mapping For 4D Dose Accumulation: Fundamental Differences and Dosimetric Consequences. Phys Med Biol 2014;59:173-88.
28. Chui CS, Yorke En, Hong L. The effects of intra-fraction organ motion on the delivery of intensity-modulated field with a multileaf collimator. Med Phys 2003;30:1736-46.
29. Jiang SB, Pope C, Al Jarrah KM, et al. An experimental investigation on intra-fractional organ motion effects in lung IMRT treatments. Phys Med Biol 2003;48:1773-84.
30. Schaefer M, Münter MW, Thilmann C, et al. Influence

of intrafractional breathing movement in step-and shoot IMRT. Phys Med Biol 2004;49:N175-9.
31. Kardar L, Li Y, Li X, et al. Evaluation and mitigation of the interplay effects for intensity modulated proton therapy for lung cancer in a clinical setting. Pract Radiat Oncol 2014;4:e259-68.

doi: 10.21037/jxym.2018.11.04
Cite this article as: Phua JH, Ang KW. Interplay effect in lung cancer proton therapy. J Xiangya Med 2018;3:43.

